The Diffuse Plate boundary of Nubia and Iberia in the Western Mediterranean: crustal deformation evidence for viscous coupling and fragmented lithosphere

Mimmo Palano [a], Pablo J. González [b], José Fernández [c]

[a] Istituto Nazionale di Geofisica e Vulcanologia, Osservatorio Etneo - Sezione di Catania, Catania, Italy

[b] COMET. Institute of Geophysics and Tectonics, School of Earth and Environment, University of Leeds, Leeds, United Kingdom

[c] Institute of Geosciences, CSIC, UCM, School of Mathematics, Ciudad Universitaria, Madrid, Spain

Abstract

A spatially dense GNSS-based crustal velocity field for the Iberian Peninsula and Northern Africa allow us to provide new insights into two main tectonic processes currently occurring in this area. In particular, we provide, for the first time, clear evidence for a large-scale clockwise rotation of the Iberian Peninsula with respect to stable Eurasia (Euler pole component: N42.612°, W1.833°, clockwise rotation rate of 0.07 deg/Myr). We favour the interpretation that this pattern reflects the quasi-continuous straining of the ductile lithosphere in some sectors of South and Western Iberia in response to viscous coupling of the NW Nubia and Iberian plate boundary in the Gulf of Cádiz. We furnish evidence for a fragmentation of the western Mediterranean basin into independent crustal tectonic blocks, which are delimited by inherited lithospheric shear structures. Among these blocks, an (oceanic-like western) Algerian one is currently transferring a significant fraction of the Nubia-Eurasia convergence rate into the Eastern Betics (SE Iberia) and likely causing the eastward motion of the Baleares Promontory. These processes can be mainly explained by spatially variable lithospheric plate forces imposed along the Nubia-Eurasia convergence boundary.

Keywords: *GNSS velocity field, crustal rotation, quasi-continuous straining, Iberia*

1. Introduction

Two end-member approaches are usually adopted to model the deformation occurring at the lithospheric scale: the block or microplate approach and the continuum model (Thatcher, 2009). The former, which is analogous to global plate tectonics, has been widely applied to model the kinematics of deformation observed at the Earth's surface (*e.g.*, Avouac and Tapponnier, 1993). This approach emphasizes the role of the faults and discontinuous deformation in the brittle/elastic upper crust: if relative movement of rigid blocks is able to describe regional deformation, a marked

velocity gradient near major faults, where interseismic deficit accumulates, should be expected. The latter approach merges kinematics and dynamics under the assumption that the quasi-continuous straining of the ductile lithosphere controls the deformation (England and Jackson, 1989). This model usually assumes that the lithosphere is a uniform thin viscous sheet with no lateral or depth-wise variations in rheological properties. Although, rheological lateral variations can be added, the thin-sheet model assumes no depth variation of horizontal velocity and depth averaged values of stress. Resulting surface deformation is characterized by velocity gradients that usually are relatively smoothed in the absence of lateral viscosity variations. Although block and continuum models predict distinctly different deformation patterns and mechanical behavior, differences between their kinematics are ultimately gradual: as block size decreases and the number of faults increases, the block model approaches the deformation of a continuum, and the kinematic distinction between the two models becomes blurred.

The Iberian Peninsula (Fig. 1) forms the northern domain of the present-day plate boundary between Nubia (the African plate west of the East African Rift) and Eurasia in Western Mediterranean area. The GNSS (Global Navigation Satellite System) velocity field observed across this boundary (northern Morocco - southern Iberia) has been interpreted in terms of elastic block modelling (*e.g.*, Koulali et al., 2011 and references therein). However, the detection of a significant aseismic strain component (~75%; see Stich et al., 2007 for details) suggests that relevant continuum mechanics processes cannot be ruled out. To evaluate properly those processes, which could play a significant role in the distributed regional deformation, an improved spatial resolution of the GNSS ground deformation pattern is required.

To this aim, here we present an analysis based on up to 15 years of GNSS observations at more than 340 sites to produce a densely spaced velocity field for whole Iberian Peninsula and Northern Morocco. We provide evidence of ongoing processes such as i) a large-scale clockwise rotation of the Iberian Peninsula with respect to stable Eurasia which can be interpreted as due to the quasi-continuous straining of the ductile lithosphere, and ii) a fragmentation of the western Mediterranean basin into several crustal blocks according to their distinct geological history.

2. Background setting

2.1 Kinematics setting

The movement and deformation of the Iberian Peninsula, one of the puzzling micro-plates located along the Eurasia-Africa plate boundary, has been extensively investigated by several geological and geophysical approaches. Although no consensual geodynamic model has yet been

achieved, these approaches coupled with studies related to large scale relative plate motions have shown that the current tectonic plate setting of the Iberian Peninsula has changed significantly over geological time (*e.g.*, Roest and Srivastava, 1991; Rosenbaum et al., 2002; Platt et al., 2013). In late Paleozoic times, after the Hercynian orogeny, the Iberian Peninsula was part of Pangea. Soon after the Atlantic Ocean rifting episode (~180 Ma ago), the northward propagation of the rifting process produced the eastward movement of Africa relative to Iberia-Europe and the opening of the transtensional Atlas and Betic-Rif basins (connecting the Atlantic to the Ligurian-Tethys oceanic domains) in early and middle Jurassic times respectively (Vergés and Fernàndez, 2012 and reference therein). In early Cretaceous times, the northward propagation of the Atlantic Ocean spreading along the western margin of Iberia produced the abandonment of the Ligurian-Tethys corridor and the opening of the Bay of Biscay along the already rifted Pyrenean basin with a concurrent counter-clockwise rotation of the Iberian Peninsula (*e.g.*, Gong et al., 2009; Vissers and Meijer, 2012). The progressive propagation toward north of the North Atlantic led to the abandonment of the Bay of Biscay-Pyrenean opening near the early-Late Cretaceous boundary. The Iberian Peninsula behaved as an independent micro-plate until Late Cretaceous, when Africa started to move north and northwestward relative to Eurasia (the so called Alpine Orogeny; Moores et al., 1998) The northward motion of Africa squeezed the Iberian Peninsula, producing the Pyrenees orogenic chain along its northern margin and the Betic-Rif orogen along its southern boundary. Most of the Pyrenean shortening was completed by middle Oligocene times and from this time onward the convergence of Africa was mostly accommodated across the Atlas systems (North Africa), the Betic-Rif orogenic system and within the Iberian Peninsula. The interior of the Iberian plate was deformed, inverting all previously rifted regions and producing intraplate mountain ranges (*e.g.*, Casas-Sainz and de Vicente, 2009; Gibbons and Moreno, 2002). The present-day plate tectonic arrangement was reached only in the earliest Miocene, when the Iberian northern plate boundary became extinct and the peninsula became a stable part of the Eurasian plate. A tranpressive fault zone, connecting the Açores trans-tensional triple junction through the Gibraltar Orogenic Arc to the Rif and Tell-Atlas then became the main plate boundary between Africa and Eurasia in the Western Mediterranean region (*e.g.*, McKenzie, 1970; Andrieux et al., 1971; Meghraoui and Pondrelli, 2012).

2.2. Seismotectonic setting

The occurrence of several large earthquakes (with estimated magnitude M≥6) in the last millennium on the studied area is well documented in the historical records (Fig. 2a; Stucchi et al., 2013; www.emidius.eu/SHEEC/sheec_1000_1899.html). The Lisboan area has been hit by large

earthquakes (M≥6.4) in 1344, 1531, 1858 and 1903, while the November 1, 1755 (M_w=8.7) and the February 28, 1969 (M_w=8.0) earthquakes, both striking the Gulf of Cádiz (Fig. 2a), were the largest historical events occurred in the region. Other large earthquakes (M≥6.4; Stucchi et al., 2013) are located along the Betics in southern Iberia (*e.g.*, 1522, 1680, 1748, 1829, 1884, and 1954) along northern Morocco (1079, 1623, 1624, 1909 and 2004) and along northern Algeria (1365, 1716, 1819, 1825, 1858, 1867, 1891, 1910, 1922, 1954, 1980 and 2003). Large earthquakes (M≥6.0) occurred also along the Pyrenees in 1373, 1428 and 1660 (Stucchi et al., 2013).

Since 2000, more than 5300 earthquakes with magnitude M≥2.5 were located in the NW Africa-Iberia area. Considering the distribution of instrumental seismicity (Fig. 2a), it is well documented that all the borders of the Iberian Peninsula are characterized by a diffuse seismicity, while on the central sector of the peninsula seismicity wanes. The bulk of instrumental seismicity is concentrated along the WSW-ENE regional-scale structures in northern Algeria and the easternmost Atlantic Ocean (Gulf of Cádiz), well marking two segments of the Nubia-Eurasia plate boundary. In northern Algeria, earthquakes have hypocentral depths shallower than 20 km and are characterized by fault plane solutions with prevailing reverse and subordinately strike-slip faulting style (Fig. 2a,b). In the Gulf of Cádiz, earthquakes have intermediate hypocentral depths and are characterized by fault plane solutions having reverse and strike-slip features (Fig. 2a,b). Across the Gibraltar Orogenic Arc, the majority of shallower earthquakes are concentrated in the Betics and Rif mountain belts. Seismicity at intermediate-depth is concentrated along a mainly N-S trend spanning the Alboran Sea and dipping southward from crustal depths beneath the Betics to a depth of ~150 km beneath the basin centre. Occasional very deep and large magnitude earthquakes (~650 km) occur under the Central Betics (Buforn et al., 2004).

3. GNNS data processing and velocity field computation

Here we analyze an extensive GNSS dataset covering approximately 15 years of observations, from 1999.00 up to 2014.68, at all continuous sites where data are openly shared. The dataset includes 280 continuous GNSS sites available at the EUREF Permanent Network (www.epncb.oma.be), at the Crustal Dynamics Data Information System (http://cddis.nasa.gov) and from various networks developed on the Iberian Peninsula by local institutions and agencies mainly for mapping, engineering and cadastral purposes. In addition to continuous GNSS sites, we included data from 25 episodic GNSS sites located in Morocco (see Koulali et al., 2011 for details) with surveys spanning the 1999.80-2006.71 time interval, whose raw observations are available through the UNAVCO archive (www.unavco.org). We have updated and extended previous studies (*e.g.*, Fernandes et al., 2007; Koulali et al., 2011; Palano et al., 2013; Echeverría et al., 2013; Gárate

et al., 2014) with more than 110 new stations having times series longer than 2.5 years, especially from Portugal, northern Iberia and western Pyrenees. The GNSS data were processed by using the GAMIT/GLOBK software (www-gpsg.mit.edu), by adopting the strategy described in Appendix A of the Supplementary material section (see also Palano, 2015 for additional details). By using the GLORG module of GLOBK, all the GAMIT solutions and their full covariance matrices are combined to estimate a consistent set of positions and velocities in the ITRF2008 reference frame (Altamimi et al., 2012).

To improve the detail of the geodetic velocity field over the studied area, we perform a rigorous integration of our solutions with those reported in Serpelloni et al. (2007), Koulali et al. (2011), Echeverría et al. (2013) and Gárate et al. (2014). In particular, since our solutions and the published ones share several common stations, we aligned their velocities to our ITRF2008 solution by applying a Helmert transformation, obtained by solving for the transformation parameters that minimize the RMS of differences between velocities at common sites. The average discrepancies are small, and the RMS velocity difference for the common stations is less than 0.4 mm/yr. The resulting velocities and their 1σ uncertainties, aligned to the ITRF2008 are reported in Table S1.

To adequately show the crustal deformation pattern over the investigated area, we align our ITRF2008 GPS velocities to a fixed Eurasian reference frame (Cannavò and Palano, 2015; see also Table S1 and S2 of the supplementary material section). The resulting velocity field, with error ellipses at the 95 per cent confidence level, is shown in Fig. 3.

It is well regarded that the formal, standard error of the GNSS solution underestimates the true uncertainty in the GNSS velocities. Roughly speaking, the error spectrum for most stations is usually represented by a combination of seasonal signal, white noise and flicker noise (see supplementary material for details). To properly infer valuable information about the crustal motion currently occurring on the studied area, the noise effects on velocity estimates need to be taken into account. To this aim, we account for temporally correlated noise in each continuous GNSS time series by using the first-order Gauss-Markov extrapolation (FOGMEX) algorithm proposed by Herring (2003) to determine a random-walk noise term, which we then incorporated into the Kalman filter used to estimate the velocities. For the episodically measured sites, a random-walk of 1.5 and 2.5 mm $yr^{-0.5}$, representing the average values obtained for all continuous GNSS stations analyzed in this study, were added to the assumed error in horizontal and vertical positions, respectively. The adopted strategy is described in detail in the Supplementary material section (Appendix A).

Moreover, the simple visual inspection of velocity field reported in Fig. 3 evidences that some stations show random velocities (differences of about 0.5-1 mm/yr) with respect to nearby sites.

This aspect could be mainly related to the monument instability of the station. In particular, a number of the analyzed GNSS networks has been developed to support commercial applications, such as mapping and cadastral purposes and stations are characterized by a wide variety of different monument types. Pillars, or steel masts, anchored to buildings represent the largest number, while monuments directly founded on consolidated bedrock are present in minor percentage. Hence, the observed geodetic monument instability is due to varying conditions of the anchoring media (*e.g.*, soil, bedrock, building, etc.) coupled with local processes (*i.e.*, soil humidity content, water table level changes, bedrock thermal expansion, etc.).

4. Results

The dense spatial coverage of our geodetic velocities, comprising over 380 stations, allow us to detect for the first time a significant large-scale clockwise rotation of the southern (*i.e.*, central and western Betics) and the western (*i.e.*, western Portugal) sectors of the Iberian Peninsula. In particular, the stations located in central and western Betics move toward WSW with rates of ~1.1 mm/yr; the stations located in SW Iberia moves mainly toward NW with rates of ~3 mm/yr, while stations located in central and northern Portugal move northwards with rates of ~1 mm/yr. The spatially smooth SW-Iberia clockwise crustal deformation pattern suggests a rigid rotating lithosphere block. Therefore, to test such hypothesis, we estimated the Euler vector components (latitude and longitude of pole, rotation rate) for the Iberian block by using the PEM2 software (Cannavò and Palano, 2015). We started by solving for Iberia's angular velocity w.r.t. the fixed Eurasian reference frame considering a total of 229 GNSS sites distributed over the whole Iberian Peninsula with the exclusion of sites located on Baleares and south-eastern Betics because their proximity to active faults. Then, we estimated recursively the Euler vector components for the Iberian block by excluding all the stations rejecting the null hypothesis based on the F-ratio criteria (see Appendix A of the Supplementary material section and Table S2). A final set of 189 sites infer a pole (N42.612°, W1.833°) that is located closely to the northwestern sector of the Pyrenean mountain range and is characterized by a clockwise rotation rate of 0.07 deg/Myr (Fig. 3). No significant residuals remain in the pole computation; ~80% of the 189 sites show residuals lower than 0.75 mm/yr, evidencing that the estimated pole reasonable describes the observed geodetic velocity field.

Eastern Betics (*e.g.*, Almería-Murcia region) show a deformation pattern that strongly differs from the one observed for surrounding areas. In particular, geodetic velocities clearly show a NW-to-NE fan-shaped pattern with rates ranging from ~3 mm/yr near the coast to ~0.8 mm/yr inland (Fig. 3). The Baleares promontory shows a motion that is comparable with the one detected by

easternmost stations located on Eastern Betics but differs from the one observed along the Catalan coastal range (northeastern Iberia) suggesting the possible presence of a distributed shear zone on the Valencia trough accounting for a general left-lateral motion (Fig. 3).

Stations located on the southern sector of Betics moves toward SW; this, coupled with the NW motion of stations located in eastern Rif clearly, depicts a NNW-SSE to N-S contraction of the Alboran Basin. Moreover, the western sector of the Alboran Basin seems subject to an E-W elongation due to the westward motion of stations located on the central sector of the Gibraltar Arc. A differential motion of ~0.3 mm/yr between the stations located externally and internally this area can be recognized, resulting into a minor E-W contraction of the arc (Fig. 3).

5. Discussion

In the following we discuss the main findings and their implications for regional and local deformation processes.

5.1. Large-scale clockwise rotation of the SW and W boundaries of Iberian Peninsula

As previously described, stations located in south-western and western Iberia show a characteristic and significant pattern of motion, while stations installed in the remaining part of Iberia lack any significant residual motion with respect to stable Eurasia. This last feature has been observed in previous GNSS-based studies estimating the Euler pole parameter for the Eurasian Plate (*e.g.*, Nocquet and Calais, 2003; Altamimi et al., 2012; Palano et al., 2013), while the large-scale clockwise rotation of southern and western Iberia has been never identified due to the limited coverage of GNSS stations on these areas in the past, and eventually due to the small magnitude of the crustal deformation.

In the previous section, we reported that stations located along southern and western Iberia can be represented with a clockwise rotating rigid block model. This large-scale rotation is consistent with those detected by paleomagnetic measurements in Neogene sedimentary basins located in the central and western Betics (*e.g.*, Mattei et al., 2006 and references therein) while is two orders of magnitude smaller than those estimated by Meghraoui and Pondrelli (2012) along the NW Africa - Iberia plate boundary. However, the northern and eastern borders of an Iberian block cannot be clearly determined, nor does the current seismicity seem to indicate clear styles of deformation at its edges. Therefore the limits of such lithospheric block are not clear, and perhaps not represented as sharp fault bounding systems. An hypothesis would be to expect that the observed block comprises the whole Iberian Peninsula (as a microplate). However, a rotating rigid block model would predict

significant shortening and left-lateral shear along the Western (off-shore Lisbon) and pure shortening at the North Iberian margin (uplift of the Cantabrian Mountains and North Spain Hercynian Massif plateau?). In addition, an Iberian rotating block would require S to W motion of NE and Eastern sectors of the Iberian Peninsula (Catalonia, Aragon and Valencia), which currently velocities in this section behave consistently with respect to stable Eurasia within the error ellipses. This suggests that despite the good agreement of the best-fitting model provided by our estimated pole, a rigid rotating block with net (fault bounded) limits is unlikely to fully explain the deformation process in SW and Western Iberia as a whole. Alternatively and or in addition, the lithosphere is likely undergoing distributed deformation in some sectors of south and western Iberia, and/or unknown off-shore margin structures (e.g., Gulf of Cádiz) would be currently accumulating significant interseismic strain.

In Fig. 4 we applied a median filter to all stations within 1x1 degree grid in order to better highlight this pattern (gray vectors). We filter the velocity field by computing the median value location of all stations to represent the vector position, and then vector magnitudes corresponding to the median values of East-West and North-South components of the velocity field for all stations within a grid cell. Fig. 4 shows a representation of the interaction between the Nubia-Eurasia convergence and the residual motion w.r.t. Eurasia of the SW and W stations in Iberia. The different predicted vectors (blue arrows) differ significantly for the expected relative convergence motion between Nubia and Eurasia plates (red arrows). Moreover, we note that the azimuth of small circles around both poles, and hence the predicted motion, aligned along a NE-SW striking line crossing central Spain. This direction intersects the Nubia-Eurasia plate boundary around the Gulf of Cádiz (west of Gibraltar to the Gorringe Bank). However, the magnitude of the vector velocities disagrees by about 60%. This feature can be interpreted as the result of a significant viscous coupling of the Nubia-Eurasia convergence motion around the Gulf of Cádiz plate boundary region. In Fig. 5a and 5b, a SW-NE profile showing perpendicular motion component of stations from South-western Iberia to NE Spain shows a characteristic decay, which could be consistent with models of parallel velocity over wide shear strain-rates of continental deformation (*e.g.*, England et al., 1985; Whitehouse et al., 2005). Such models predict an approximate exponential decay away from the plate boundary ($V_y \simeq V_o e^{-x/\lambda}$), with a length scale $\lambda \sim L/(2\pi\sqrt{n})$, where L is the finite length of plate boundary and n is an exponent that synthesizes the characteristics of a power-law rheology of the continental lithosphere.

As we estimated previously the only plate boundary segment with parallel vectors for the SW Iberia pole and the Nu-Eu pole is the Gulf of Cádiz region (Fig. 4). Therefore, we can assume that the Gulf of Cádiz is the most important segment imposing parallel traction to the plate boundary,

and we limit its dimensions from the Gibraltar Strait to the Gorringe Bank, with a maximum length of 450 km. As seen in Fig. 5a, this model is a first order approximation consistent with the observed velocity pattern. Exploring the parameters of this expression to fit the observed velocities along the selected profile, suggest that n is poorly constrained within values ranging from n=1 to n=10. In general, if n increases the model predicts shorter L distances (L≤100 km). Although, L can be numerically small to obtain decay rates consistent with the observed parallel velocities, we favor a longer segment to explain the observed velocity decay not only in the analyzed profile but also as an explanation for most SW Iberia region. An alternative is to consider a box-car boundary condition for the applied tangential plate boundary force. Such boundary conditions decrease significantly the length scale as $\lambda = L/(4\sqrt{n})$, (Whitehouse et al., 2005). Consequently, the power-law index needed to fit the observations increases to n ~ 3-5 for reasonable L values (~400-500 km). We acknowledge, however, that a wide range of model parameters can be chosen to fit the observations (Fig. 5c and 5d).

The main difficulty to constrain the model parameter space is the possible interactions with the Alborán block and the lack of observations near the expected plate boundary at the Gulf of Cádiz, *e.g.*, the SWIM structure (Zitellini et al., 2009), in an offshore region. Indeed, the observations along the profile coincide with the length scales for which the exponential decay resembles, within the observed errors, a linear decay. As a result, the current observations still not completely unique to reject rigid block rotations. Moreover, it is plausible that both processes coexist to explain the observed perpendicular velocity decay (Fig. 5a), with a long-wavelength linear trend from an inferred Iberian rotation block superimposed to the near plate boundary shear drag. Therefore, to solve this question future seafloor geodetic observations must be considered. In addition, more advanced two-dimensional physical modeling is currently under development to gain insights of the whole pattern of observations of this complex plate boundary. Although non-unique, simulations based on reasonable values, as shown above, suggest that observations can be partially explained using a simple physical model, without invoking undefined lithosphere block fault/deformation systems.

5.2. Crustal motion of the Baleares promontory

Another interesting feature well recognized on the dense geodetic velocity field is the different motion between the Baleares promontory (BalP in Fig. 1) and the Catalan coastal range (NE Iberia, CCC in Fig. 1) that suggests the presence of a shear zone on the Valencia Trough accounting for a left-lateral motion (Fig. 6). Seismic reflection profiles and bathymetric surveys carried out across the whole Valencia Trough have highlighted the presence of some extensional faults along the

Catalan coastal range and the northwestern margin of the trough and contraction structures along the Baleares promontory (*e.g.*, Perea et al., 2012). Geological evidence of Holocene activity on these faults suggests that they can accommodate the observed left-lateral motion between the Baleares promontory and the Catalan coastal range (Perea et al., 2012). Moreover, the observed ENE motion of the Baleares promontory seems to be related to the present-day Eastern Betics deformation process (see section 5.3.), therefore suggesting a structural and kinematic linkage with the left-lateral strike-slip Trans-Alboran Shear Zone, a NE-SW trending tectonic lineament that cuts across the southeastern margin of the Iberian Peninsula, through Eastern Betics, and crosses the Alboran Basin (Fig. 6). Since stations located on the Sardinian-Corsica block show no significant residual motion with respect to stable Eurasia (see Palano, 2015), this motion seems to be entirely absorbed within the Liguro-Provençal basin. Furthermore, the differential motion between the Baleares promontory and the northern Algerian margin suggests that a small fraction of the general NW-SE Iberia-Nubia oblique convergence could be absorbed as right-lateral motion along the NE-SW-oriented Emile Baudot Escarpment (EBE in Fig. 6), which is considered as the surface expression of a lithospheric right-lateral strike-slip fault system related to the boundary between the continental crust of the Baleares promontory and the thin oceanic crust of the Algerian basin (Acosta et al., 2002; Mauffret et al., 1992). Such a right-lateral motion is clearly recognized also when the velocity field is referred to the Nubia plate (see Fig. S2 in the supplementary material), since the motion of the Baleares promontory show an oblique relationship (~80°) with respect to the average strike (~N40°E) of the Emile Baudot Escarpment. Based on the simple vectorial decomposition of the velocities, referred to both Nubia and Eurasia reference frames, of stations located on western and central Balearic, we estimated a right-lateral motion ranging in between 0.8 - 1.5 mm/yr. Additionally, a differential motion among the islands of the promontory, related to a right lateral motion on an en-echelon array of NW-SE faults cross-cutting the promontory (*e.g.*, Acosta et al., 2002; Sánchez-Alzola et al., 2014) can be recognized (Fig. 6). All these features, coupled with the presence of inherited lateral lithospheric shear structures (*e.g.*, Sanz de Galdeano, 1990 and references therein) lend credit to a crustal segmentation of this sector of the Mediterranean Sea.

5.3. Crustal deformation of Betics

Eastern Betics are characterized by geodetic velocity vectors arranged into a WNW-to-NE fan-shaped pattern (Fig. 6). This pattern, which was previously described in Echeverría et al. (2013), depicts a prevailing NNW-SSE crustal contraction of the area in agreement with the main

thrusting regime inferred by geological and seismological observations (*e.g.*, Palano et al., 2013; González et al., 2012, and reference therein; Fig. 2).

The contraction seems accommodated by a diffuse array of left-, right-lateral strike-slip and reverse faults, belonging to the "Trans-Alboran" and "Eastern Betics" shear Zones (e.g. Carboneras fault, Palomeras fault, Alhama de Murcia fault; see Echeverría et al., 2013 for additional details). We suggest that such crustal contraction is related to an independent tectonic block which, trapped within the Nubia-Iberia collision, transfers a fraction of the convergent rate occurring along the westernmost Algerian margin (Oran-Chlef region; Fig. 6) into Eastern Betics. The lack of high quality P-wave tomography extensively covering the area does not allow us to put constraints on its size and shape, however recent geological and geophysical data collected along the southern margin of the Algerian basin clearly show the existence of an independent oceanic-type crustal block (Medaouri et al., 2014).

Another interesting feature recognized in our geodetic velocity field is the sharp change in velocities of central Betics with respect to easternmost Betics which depicts a westward relative motion of the former area and induces a crustal extension closely to Sierra de Filabres - Almería regions (Fig. 6). This extension pattern have prevailing E-W features and well agree with normal faulting inferred by mapped normal faults (Sanz de Galdeano et al., 2012) and focal mechanism solutions (see Fig. 2b for details), both having planes with prevailing N-S attitude. This extensional area has been recently indicated as the eastern edge of a crustal block which is affected by delamination processes by De Lis Mancilla et al., (2013). These authors indicated the external front of Betics as the northern boundary of this crustal block, however our data suggests that ~2 mm/yr of differential right-lateral motion appear to be accommodated within this block, along an E-W trans-tensional deformation zone connecting the Sierra Nevada region to Cádiz across the Granada Basin and the external Betics (Martìnez-Martìnez et al. 2006). The western sector of this E-W trans-tensional deformation zone spatially agrees with the northern boundary of a much larger Alboran block proposed by Koulali et al. (2011).

5.4. Crustal deformation of Alboran Basin

As can be observed in Fig. 3 the Alboran Basin is not directly sampled by geodetic observations, but valuable information can be inferred by considering the motion of bordering stations. In particular, considering the stations located along southern Betics and north-eastern Rif a NNW-SSE to N-S contraction at a rate of ~3.4 mm/yr of the Alboran Basin can be recognized. This contraction is coherent with long-term geological observations and geodynamic reconstructions of tectonic processes affecting this area and with the current Nubia-Eurasia convergence-rate (Fig. 4

and pole of rotations in Table S1). In particular, several studies have pointed out that a prevailing NNW-SSE contraction involving the entire basin and producing reverse and strike-slip faulting and related folding, started since about 8 Myr (Bourgois et al., 1992; Campos et al., 1992; Comas et al., 1999; Morel and Meghraoui, 1996). The tectonic activity of the Alboran Basin is proved by instrumental and historical earthquakes (Fig. 2; Palano et al., 2013 and references therein). Indeed, the occurrence of moderate to high magnitude earthquakes characterized by a mixture of fault plane solutions (from reverse to strike-slip to normal faulting) suggests that the general NNW-SSE to N-S contraction is currently partitioned by some primary crustal/lithospheric tectonic structures (*e.g.*, Trans-Alboran Shear Zone, Yusuf Fault, Fig. 6). In addition, the differential motion between stations located along the internal zones of the Gibraltar Arc (*e.g.*, northern and central Rif) w.r.t. those located along the northern (*e.g.*, southern Betics) and southern (*e.g.*, Al-Hoceima - Melilla region) boundaries of the Alboran Basin indicate ~2.4 mm/yr of E-W crustal stretching of the western side of the basin. The intra-basin extension is coupled with a ~0.3 mm/yr differential motion observed between the stations located externally and internally the central sector of the Arc, which defines a gentle E-W contraction of this sector of the Arc. Overall, this pattern indicates a clockwise rotation of the western sector of the Alboran Basin and surrounding parts of the Betics and Rif domains, which began more clearly when the velocity field is referred to the Nubia plate (see Fig. S2 in the supplementary material) as already evidenced in Koulali et al. (2011). Along the NW Nubian margin, the westward motion of the Gibaltar Arc decreases toward the south near the boundary of the Atlas system while it is abruptly confined westward by the Nekor fault, an active NE-SW left-lateral strike slip fault representing the southwestern end segment of the Trans-Alboran Shear Zone (Fig. 3). Eastward of the Nekor fault the geodetic velocity field is characterized by vectors ~NW-oriented, indicating a convergence rate ranging from 2.5 mm/yr to 5 mm/yr across the plate boundary between Iberia and Morocco-Algeria regions in agreement with previous estimations (*e.g.* Meghraoui and Pondrelli, 2012 and references therein).

6. Conclusions

The spatially dense crustal velocity field reported here allowed us to provide new insights into the crustal tectonic processes currently occurring in the western Mediterranean Sea. At least two main tectonic processes can be identified (Fig. 7):

1) We detected a slow large-scale clockwise rotation (~0.07 deg/Myr) of the Iberian Peninsula w.r.t. a pole located closely to the northwestern sector of the Pyrenean mountain range. Although this crustal deformation pattern could suggest a rigid rotating lithosphere block,

this model would predict significant shortening along the Western (off-shore Lisbon) and North Iberian margin which cannot totally ruled out but currently is not clearly observed. Conversely, we favour an interpretation that this pattern partially reflects the quasi-continuous straining of the ductile lithosphere of south-western and the western Iberia in response to viscous coupling of the mainly right lateral shear Nubia-Iberia plate boundary along the Gulf of Cádiz segment (n ~ 1-3.5 for the lithosphere rheology and L ~ 350-500 km, Gulf of Cádiz segment), possibly superimposed on an even slower rotation-rate of Iberia.

2) The western Mediterranean basin appears fragmented into independent crustal tectonic blocks, which trapped within the Nubia-Eurasia collision, are currently accommodating most of the plate convergence rate. Based on geophysical and geological observations, these blocks are characterized by continental-type (Valencia Trough and Baleares Promontory; Pascal et al., 1992), transitional-type (Alboran block; Comas et al., 1999; Torné et al., 2000) and oceanic-type crust (oceanic western Algerian Block; Medaouri et al., 2014). The blocks are delimited by inherited lithospheric shear structures (*e.g.*, Acosta et al., 2002). Among these blocks, the (oceanic western) Algerian one is currently acting as an indenter, transferring a fraction of the convergent rate into Eastern Betics and likely causing the eastward motion of the Balearic Promontory.

Most of the observed crustal ground deformation can be attributed to processes driven by spatially variable lithospheric plate forces imposed along the Nubia-Eurasia convergence boundary. Nevertheless, the observed deformation field infers a very low convergence rates as observed also at the eastern side of the western Mediterranean, along the Calabro Peloritan Arc, by space geodesy (Palano, 2015).

Acknowledgements

PJG would like to thank Tim Wright, Richard Walters, Greg Houseman and Liam Finnerty for long and stimulating discussions. Critical comments by John Platt and Mustapha Meghraoui greatly improved the quality of this manuscript. We thank all individuals and institutions for maintain the network and providing free access to GNSS data: ARAGEA (http://gnss.aragon.es), BIGF (www.bigf.ac.uk), Biscay (www.bizkaia.net), CANTABRIA (www.gnss.unican.es), CATNET (catnet-ip.icc.cat), ERVA (www.icv.gva.es), EUREF (www.epncb.oma.be), EUSKADI (www.gps2.euskadi.net), GALNET (www.cartogalicia.com), Gipuzkoa (http://b5m.gipuzkoa.net),

HUESCA (http://epsh.unizar.es), ICM (http://www.madrid.org/cartografia/planea/cartografia/html/web/VisorGps.htm), IDE (http://www.iderioja.larioja.org), IGN (www.ign.es), Itacyl (http://gnss.itacyl.es/), RAP (www.ideandalucia.es), REGAM (http://cartomur.imida.es/regam), Region de Murcia (http://gps.medioambiente.carm.es), ReNEP (www.igeo.pt), REP (www.rep-gnss.es), RGAN (www.navarra.es), RGP (http://rgp.ign.fr), SOPAC (http://sopac.ucsd.edu/), UNAVCO (www.unavco.org), XGAIB (http://xarxagnss.caib.es). XGAIB network is managed by SITIBSA (Servei d'Informació Territorial de les Illes Balears) Conselleria d'Agricultura, Medi Ambient i Territori (Govern de les Illes Balears). This work has been supported by the Spanish MINECO research projects AYA2010-17448 and ESP2013-47780-C2-1-R. It is a contribution for the Moncloa Campus of International Excellence.

Figure Captions

Figure 1. Simplified tectonic map of western Mediterranean showing the main geological and structural features of Eurasia and Nubia plates. Mapped faults are redrawn from Acosta et al., (2002); Asensio et al. (2012); García-Mayordomo et al. (2012), Meghraoui and Pondrelli, (2012); Palano et al. (2013). Abbreviations are as follows, reporting location of major basins: Liguro-Provençal (LPB), Algero-Balearic (ABB), Alboran (AB), Valencia Trough (ValT); Massifs: Hercynian (HerM) and Morrocan Meseta (MM); Mountain Belts: Cantabrian Mountains (CanMt), Costero-Catalan Chain (CCC), Iberian Chain (IbC), Pyrenees, Atlas, Tell, Rif and Betics; Oceanic-Continent domains: Galician Bank (GaB), Gorringe Bank (GoB), Horseshoe Bank (HoB) and Gulf of Cádiz (GC); Fragmented blocks: Baleares Promontory (BalP) along Emile Baudot Escarpment (EBE), and Sardinian Corsica block (SC), and major plate boundary structures: Gloria Fault and Algerian margin. Colours and patterns represent different rock ages: 1. Neoproterozoic, 2. Paleozoic, 3. Mesozoic, 4. Tertiary-Quaternary basins, and OC, Oceanic crust.

Figure 2. a) Historical earthquakes (with estimated magnitude M≥5; www.emidius.eu/SHEEC/sheec_1000_1899.html; Stucchi et al., 2013) occurred in the last millennium are reported as blue and yellow squares, for 1000 - 1899 and 1900 - 1999 time intervals, respectively. Instrumental seismicity (from 2000 up to date; www.ign.es), sized as a function of magnitude and classified with different colors as a function of the focus depth, is reported as points. b) lower hemisphere, equal area projection for fault plane solutions with magnitudes of between 3.0

and 8.0; FPSs are colored according to rake: red indicates thrust faulting, blue is normal faulting, and yellow is strike-slip faulting.

Figure 3. GNSS velocities and 95 per cent confidence ellipses in a fixed Eurasian reference frame (see Supplementary Material for details).

Figure 4. Gray arrows represent smoothed velocities obtained by applying a median filter to all stations within 1x1 degree grid. Blue and red dashed lines represent small circles around the location of the estimated pole of rotations corresponding to the virtual Iberia w.r.t. Eurasia (blue) and Nubia w.r.t. Eurasia (red) poles. Predicted GNSS velocity vectors are show for points along the approximate location of the plate boundary (blue Iberia-Eurasia virtual pole, and red Nubia-Eurasia pole). Note that the azimuth of the small circles, and hence the predicted motions are only aligned on a virtual line that crosses central Spain striking N30°E direction, and cutting the Nubia-Eurasian plate boundary around the Gulf of Cádiz. However, the magnitudes of the blue and red vectors disagree by about 60%. Orange lines show a simplified plate boundary.

Figure 5. a) NE-SW profile perpendicular velocity from the pole of rotation in stable undeformed Iberia interior the pole of rotation in to the plate boundary limit at SW Iberia (Gulf of Cádiz). Gray dots are original observed profile-parallel velocity. Black dots spatially filtered median observations. Red line is a model using box-car plate boundary condition with Vo=5 mm/yr, L=350 km, n=2.5. Blue line represents the predicted perpendicular velocities from the estimated Iberian rotation pole model. b) Map showing the location of the selected profile (blue line). The end points of the selected profile were selected to match the inferred Iberian Euler pole and the inferred Nubia-Eurasia plate boundary zone. c) Misfit (mm/yr) plot as a function of half-wavelength, L and n power-law index for the case of homogeneous boundary condition. d) Misfit (mm/yr) plot as a function of box-car length, L and n power-law index for the case of box-car boundary condition.

Figure 6. Detail of the GNSS velocities and 95 per cent confidence ellipses in a fixed Eurasian reference frame for the Algerian margin, Eastern Betics and Baleares Promontory area. Abbreviations are: GC, Gulf of Càdiz; WAB, Western Alboran Basin; AH, Al-Hoceima; GB, Granada Basin; SN, Sierra Nevada; SF, Sierra de Filabres; TASZ, Trans-Alboran Shear Zone; EBSZ, Eastern Betics Shear Zone; YF, Yusuf Fault; EBE, Emile Baudot Escarpment.

Figure 7. Schematic model: main lithosphere domains are reported as irregular polygons with different colors. Eurasia, Nubia and Iberia are represented as large plates with continental and oceanic lithospheres domains. Eurasia and Iberia cannot be distinguished in terms of motion in the area of the Pyrenees, therefore they are shown as a single block with potentially variable strength, as shown the variable red shade. SW and Western Iberia is undergoing clockwise rotation that fades away towards North and Eastern Iberia. There are smaller domains in between the major plates, such as the Alboran one, which in currently undergoing clockwise rotation, internal deformation and contraction in the West and SW borders. Geodetic data indicates that the Baleares promontory is escaping to the NE, however its border structures still to be defined. Sardinia-Corsica block is consistent in motion with the Eurasian plate. Finally, convergence and interseismic coupling is variable along the Algerian margin, with a possible stronger oceanic lithosphere off-shore Oran (Western Algeria), which effectively transfer part of convergence into the SE Iberia (Eastern Betics).

References

Acosta, J., Muñoz, A., Herranz, P., Palomo, C., Ballesteros, M., Vaquero, M., Uchupi, E., 2001. Geodynamics of the Emile Baudot escarpment and the Balearic promontory, western Mediterranean. Mar. Petrol. Geol. 18, 349-369, doi:10.1016/S0264-8172(01)00003-4.

Andrieux, J., Fontbote, J.M., Mattauer, M., 1971. Sur un modèle explicatif de l'arc de Gibraltar. Earth Planet. Sci. Lett. 12, 191-198, doi:10.1016/0012-821X(71)90077-X.

Asensio, E., Khazaradze, G., Echeverria, A., King, R. W., Vilajosana, I., 2012. GPS studies of active deformation in the Pyrenees. Geophys. J. Int. 190, 913-921, doi:10.1111/j.1365-246X.2012.05525.x

Avouac, J.-P., Tapponnier P., 1993. Kinematic model of active deformation in central Asia, Geophys. Res. Lett. 20, 895-898, doi:10.1029/93GL00128.

Bourgois, J. A., Mauffret, A., Ammar, N. A., Demnati, N. A., 1992. Multichannel seismic data imaging of inversion tectonics of the Alboran Ridge (western Mediterranean Sea). Geo-Mar. Lett. 12, 117-122, doi:10.1007/BF02084921.

Buforn, E., Bezzeghoud, M., Udías, A., Pro, C., 2004. Seismic sources on the Iberia–African plate boundary and their tectonic implications. Pure Appl. Geophys. 161, 623-646, doi:10.1007/s00024-003-2466-1.

Campos, J., Maldonado, A., Campillo, A.C., 1992. Post-messinian evolutional patterns of the central Alboran sea. Geo-Mar. Lett. 12, 173-178, doi:10.1007/BF02084929.

543 Cannavò, F., Palano, M., 2015. Defining Geodetic Reference Frame using Matlab: PlatEMotion 2.0.
544 Pure Appl. Geophys., doi:10.1007/s00024-015-1112-z.
545 Casas-Sainz, A.M., De Vicente, G., 2009. On the tectonic origin of Iberian topography.
546 Tectonophysics 474(1-2), 214-235, doi:10.1016/j.tecto.2009.01.030.
547 Comas, M.C., Platt, J.P., Soto, J.I., Watts, A.B., 1999. The origin and tectonic history of the
548 Alboran Basin: insights from Leg 161 results. In: Zahn, R., Comas, M.C., Klaus, A. (Eds.).
549 Proceedings of the Ocean Drilling Program, Scientific Results 161, 555-580.
550 De Lis Mancilla, F., Stich, D., Berrocoso, M., Martín, R., Morales, J., Fernandez-Ros, A., Páez, R.,
551 Pérez-Peña, A., 2013. Delamination in the Betic Range: Deep structure, seismicity, and GPS
552 motion. Geology 41 (3), 307-310, doi:10.1130/G33733.1.
553 Echeverría, A., Khazaradze, G., Asensio, E., Gárate J., Martín Dávila, J., Suriñach, E., 2013.
554 Crustal deformation in eastern Betics from CuaTeNeo GPS network. Tectonophysics 608,
555 600-612, doi:10.1016/j.tecto.2013.08.020.
556 England, P., Houseman, G., and Sonder, L., 1985, Length scales for continental deformation in
557 convergent, divergent, and strike-slip environments: Analytical and approximate solutions for
558 a thin viscous sheet model. J. Geophys. Res. 90, 3551-3557, doi:10.1029/JB090iB05p03551.
559 England, P.C., Jackson, J.A., 1989. Active deformation of the continents. Annu. Rev. Earth Planet.
560 Sci. 17, 197-226, doi:10.1146/annurev.ea.17.050189.001213.
561 Fernandes, R.M.S., Miranda, J.M., Meijninger, B.M.L., Bos, M.S., Noomen, R., Bastos, L.,
562 Ambrosius, B.A.C., Riva R.E.M., 2007. Surface velocity field of the Ibero-Maghrebian
563 segment of the Eurasia-Nubia Plate boundary. Geophys. J. Int. 169 (1), 315-324, doi:
564 10.1111/j.1365-246X.2006.03252.x.
565 Gárate, J., Martín-Dávila, J., Khazaradze, G., Echeverría, A., Asensio, E., Gil, A.J., de Lacy, M.C.,
566 Armenteros, J.A., Ruiz, A.M., Gallastegui, J., Álvarez-Lobato, F., Ayala, C., Rodríguez-
567 Caderot, G., Galindo-Zaldívar, J., Rimi, A. Harnafi, M., 2014. Topo-Iberia project: CGPS
568 crustal velocity field in the Iberian Peninsula and Morocco. GPS Solutions 19(2), 287-295,
569 doi:10.1007/s10291-014-0387-3.
570 García-Mayordomo, J., Insua-Arévalo, J.M., Martínez-Díaz, J.J., Jiménez-Díaz, A., Martín-Banda,
571 R., Martín-Alfageme, S., Álvarez-Gómez, J.A., Rodríguez-Peces, M., Pérez-López, R.,
572 Rodríguez-Pascua, M.A., Masana, E., Perea, H., Martín-González, F., Giner-Robles, J.,
573 Nemser, E.S., Cabral J. and the QAFI Compilers Working Group (2012). The Quaternary
574 Active Faults Database of Iberia (QAFI v.2.0). J. Iberian Geol. 38(1), 285-302,
575 doi:10.5209/rev_JIGE.2012.v38.n1.39219.

576 Gong, Z., van Hinsbergen, D. J. J., Dekkers, M. J., 2009. Diachronous pervasive remagnetization in
577 northern Iberian basins during Cretaceous rotation and extension. Earth Planet. Sci. Lett.
578 284(3-4), 292301, doi:10.1016/j.epsl.2009.04.039.
579 González, P.J., Tiampo, K.F., Palano, M., Cannavò, F., Fernández, J. 2012. The 2011 Lorca
580 earthquake slip distribution controlled by groundwater crustal unloading. Nat. Geosci. 5, 821-
581 825, doi:10.1038/ngeo1610.
582 Herring, T.A., 2003. MATLAB Tools for viewing GPS velocities and time series, GPS Solutions, 7
583 (3), 194-199, doi:10.1007/s10291-003-0068-0.
584 Koulali, A., Ouazar, D., Tahayt, A., King, R.W., Vernant, P., Reilinger, R.E., McClusky, S.,
585 Mourabit, T., Davila, J.M., Amraoui, N., 2011. New GPS constrains on active deformation
586 along the Africa-Iberia plate boundary. Earth Planet. Sci. Lett. 308(1), 211-217,
587 doi:10.1016/j.epsl.2011.05.048.
588 Martìnez-Martìnez, J. M., Booth-Rea, G., Miguel Azanon, J. M., Torcal F., 2006. Active transfer
589 fault zone linking a segmented extensional system (Betics, southern Spain): Insight into
590 heterogeneous extension driven by edge delamination. Tectonophysics 422, 159-173,
591 doi:10.1016/j.tecto.2006.06.001.
592 Mattei, M., Cifelli, F., Martin Rojas, I., Crespo Blanc, A., Comas, M., Faccenna, C., Porreca, M.,
593 2006. Neogene tectonic evolution of the Gibraltar Arc: New paleomagnetic constrains from
594 the Betic chain. Earth Planet. Sci. Lett. 250, 522-540, doi:10.1016/j.epsl.2006.08.012.
595 Mauffret, A., Maldonado, A., Campillo, A.C., 1992. Tectonic framework of the Eastern Alboran
596 and Western Algerian basins, Western Mediterranean. Geo-Mar. Lett. 12, 104-110,
597 doi:10.1007/BF02084919.
598 McKenzie, D.P., 1970. Plate tectonics of the Mediterranean region. Nature 226, 239-243,
599 doi:10.1038/226239a0.
600 Medaouri, M., Déverchère, J., Graindorge, D., Bracene, R., Badji, R., Ouabadi, A., Yelles-
601 Chaouche, K., Bendiab, F., 2014. The transition from Alboran to Algerian basins (Western
602 Mediterranean Sea): Chronostratigraphy, deep crustal structureand tectonic evolution at the
603 rear of a narrow slab rollback system. J. Geod. 77, 186-205, doi:10.1016/j.jog.2014.01.003.
604 Meghraoui, M., Pondrelli, S., 2012. Active faulting and transpression tectonics along the plate
605 boundary in North Africa. Ann. Geophys. 55 (5), doi:10.4401/ag-4970.
606 Moores, E.M., Fairbridge, R.W. 1998. Encyclopedia of European and Asian Regional Geology.
607 Encyclopedia of Earth Sciences Series, London, 825 pp.

608 Morel, J.L., Meghraoui, M., 1996. Goringe-Alboran-Tell tectonic zone; a transpression system
609 along the Africa-Eurasia plate boundary. Geology 24 (8), 755-758, doi:10.1130/0091-
610 7613(1996)024<0755:GATTZA>2.3.CO;2.
611 Nocquet, J.M., Calais, E., 2003. Crustal velocity field of western Europe from permanent GPS array
612 solutions, 1996-2001. Geophys. J. Int. 154, 72-88, doi:10.1046/j.1365-246X.2003.01935.x.
613 Palano M., González P.J., Fernández J., 2013. Strain and stress fields along the Gibraltar Orogenic
614 Arc: constraints on active geodynamics. Gondwana Res. 23, 1071-1088,
615 doi:10.1016/j.gr.2012.05.021.
616 Palano, M., 2015. On the present-day crustal stress, strain-rate fields and mantle anisotropy pattern
617 of Italy. Geophys. J. Int. 200, 969-985, doi:10.1093/gji/ggu451.
618 Pascal, G., Torné, M., Buhl, P., Watts, A.B., Mauffret, A., 1992. Crustal and velocity structure of
619 the València trough (western Mediterranean), Part II. Detailed interpretation of five Expanded
620 Spread Profiles. Tectonophysics 203, 21-35, doi:10.1016/0040-1951(92)90213-P.
621 Platt, J. P., Behr, W. M., Johanesen, K., Williams, J. R., 2013. The Betic-Rif Arc and Its Orogenic
622 Hinterland: A Review. Annu. Rev. Earth Planet. Sci. 41, 313-357, doi:10.1146/annurev-earth-
623 050212-123951.
624 Perea, H., Masana, E., Santanach, P., 2012. An active zone characterized by slow normal faults, the
625 northwestern margin of the València trough (NE Iberia): a review. J. Iberian Geol. 38 (1)
626 2012: 31-52, doi:10.5209/rev_JIGE.2012.v38.n1.39204.
627 Roest, W.R., Srivastava, S.P., 1991. Kinematics of plate boundaries between Eurasia, Iberia and
628 Africa in the N. Atlantic from the Late Cretaceous to the present. Geology 19, 613-616,
629 doi:10.1130/0091-7613(1991)019<0613:KOTPBB>2.3.CO;2.
630 Rosenbaum, G., Lister, G.S., Duboz, C., 2002. Relative motions of Africa, Iberia and Europe during
631 Alpine orogeny. Tectonophysics, 359, 117-129, doi:10.1016/S0040-1951(02)00442-0.
632 Sánchez-Alzola, A., Sánchez, C., Giménez, J., Alfaro, P., Gelabert, B., Gil, A.J., 2014. Crustal
633 velocity and strain rate fields in the Balearic Islands based on continuous GPS time series
634 from the XGAIB network (2010-2013). J. Geod. 82, 79-8-86, doi:10.1016/j.jog.2014.05.005.
635 Sanz de Galdeano, C., 1990. Geologic evolution of the Betic Cordilleras in the Western
636 Mediterranean, Miocene to the present. Tectonophysics 172, 107-119, doi:10.1016/0040-
637 1951(90)90062-D.
638 Sanz de Galdeano, C., Garcìa-Tortosa, F.J., Pelàez J.A,, Alfaro P., Azanòn, J.M., Galindo-Zaldìvar,
639 J., Lòpez Casado, C., Lòpez Garrido, A.C., Rodrìguez-Fernàndez J., Ruano P., 2012. Main
640 active faults in the Granada and Guadix-Baza Basins (Betic Cordillera). J. Iberian Geol. 38,
641 209-223, doi:10.5209/rev_JIGE.2012.v38.n1.39215.

642 Serpelloni, E., Vannucci, G., Pondrelli, S., Argnani, A., Casula, C., Anzidei, M., Baldi, P.,
643 Gasperini, P., 2007. Kinematics of the Western Africa-Eurasia plate boundary from focal
644 mechanisms and GPS data. Geophys. J. Int. 169, 1180-1200, doi:10.1111/j.1365-
645 246X.2007.03367.x.
646 Stich, D., Martín, J.B., Morales, J., 2007. Deformación sísmica y asísmica en la zona Béticas-Rif-
647 Alborán. Revista de la Sociedad Geológica de España 20 (3-4), 311-319.
648 Stucchi et al., 2013. The SHARE European Earthquake Catalogue (SHEEC) 1000–1899. J. Seism.
649 17(2), 523-544, doi:10.1007/s10950-012-9335-2.
650 Thatcher, W., 2009. How the continents deform: the evidence from tectonic geodesy. Annu. Rev.
651 Earth Planet. Sci. 37, 237-62, doi:10.1146/annurev.earth.031208.100035.
652 Torné, M., Fernàndez, M., Comas, M.C., Soto, J.I., 2000. Lithospheric structure beneath the
653 Alboran Basin: results from 3D gravity modeling and tectonic relevance. J. Geophys. Res.
654 105 (B2), 3209-3228, doi: 0.1029/1999JB900281.
655 Vergés, J., Fernàndez, M., 2012. Tethys-Atlantic interaction along the Iberia–Africa plate boundary:
656 The Betic-Rif orogenic system. Tectonophysics, 579, 144-172,
657 doi:10.1016/j.tecto.2012.08.032.
658 Vissers, R. L. M., Meijer, P. T., 2012. Mesozoic rotation of Iberia: Subduction in the Pyrenees?.
659 Earth Sci. Rev. 110(1-4), 93-110, doi:10.1016/j.earscirev.2011.11.001.
660 Whitehouse, P.L., England P.C., Houseman, G.A., 2005. A physical model for the motion of the
661 Sierra Block relative to North America. Earth Planet. Sci. Lett. 237, 590-600,
662 doi:10.1016/j.epsl.2005.03.028
663 Zitellini, H.N., Gràcia, E., Matias, L., Terrinha, P., Abreu, M.A., DeAlteriis, G., Henriet, J.P.,
664 Dañobeitia, J.J., Masson, D.G., Mulder, T., Ramella, R., Somoza, L., Diez, S., 2009. The
665 quest for the Africa–Eurasia plate boundary west of the Strait of Gibraltar. Earth Planet. Sci.
666 Lett. 280, 13-50, doi:10.1016/j.epsl.2008.12.005.
667

Research highlights

An updated GNSS velocity field for Western Mediterranean.

Large-scale clockwise rotation of SW and W Iberian Peninsula w.r.t. Eurasia.

Fragmentation of the Western Mediterranean basin into crustal tectonic blocks.

Figure 01

Click here to download Figure: Figure_01.pdf

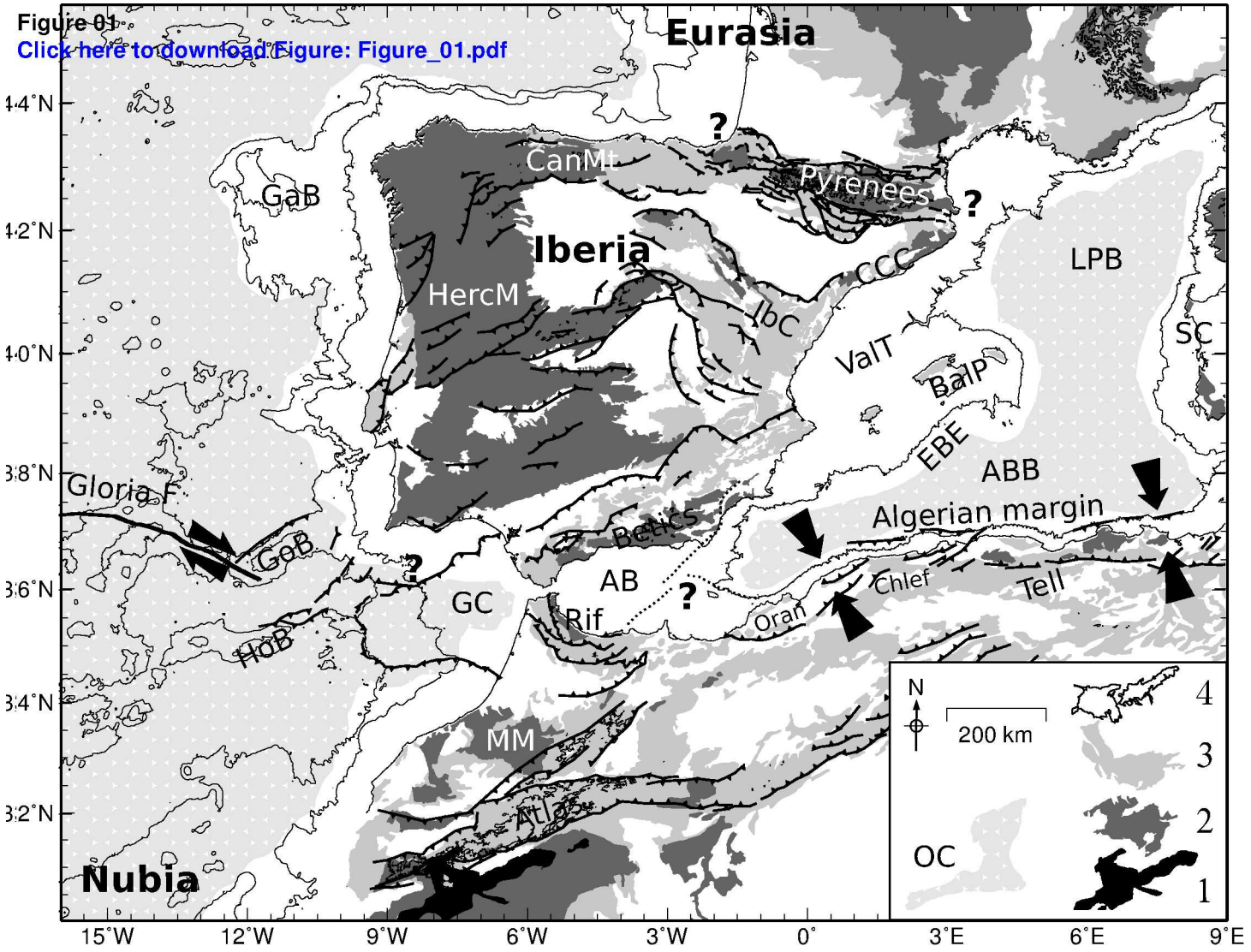

Figure 02

Click here to download Figure: Figure_02.pdf

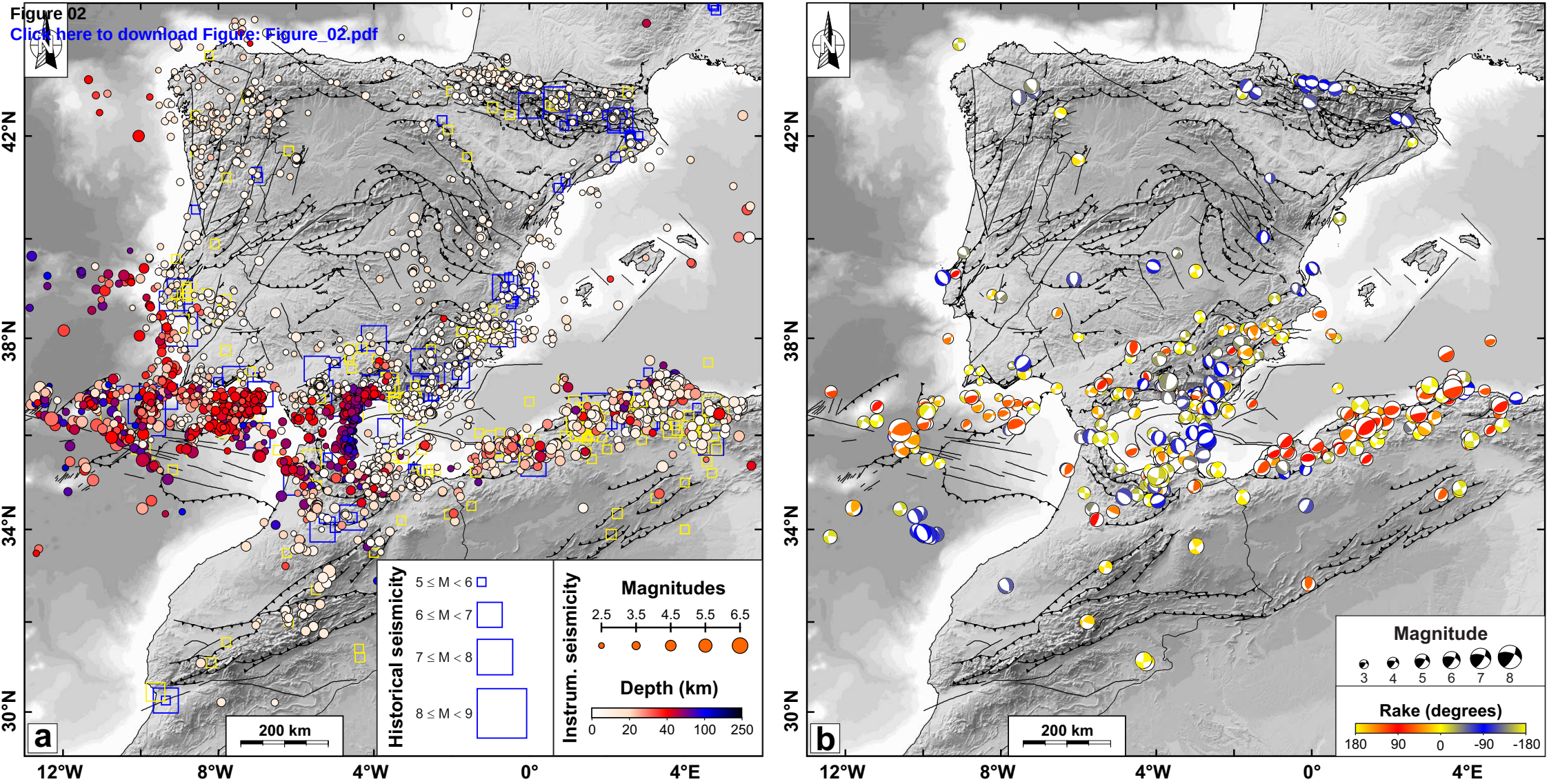

Figure 03

Click here to download Figure: Figure_03.pdf

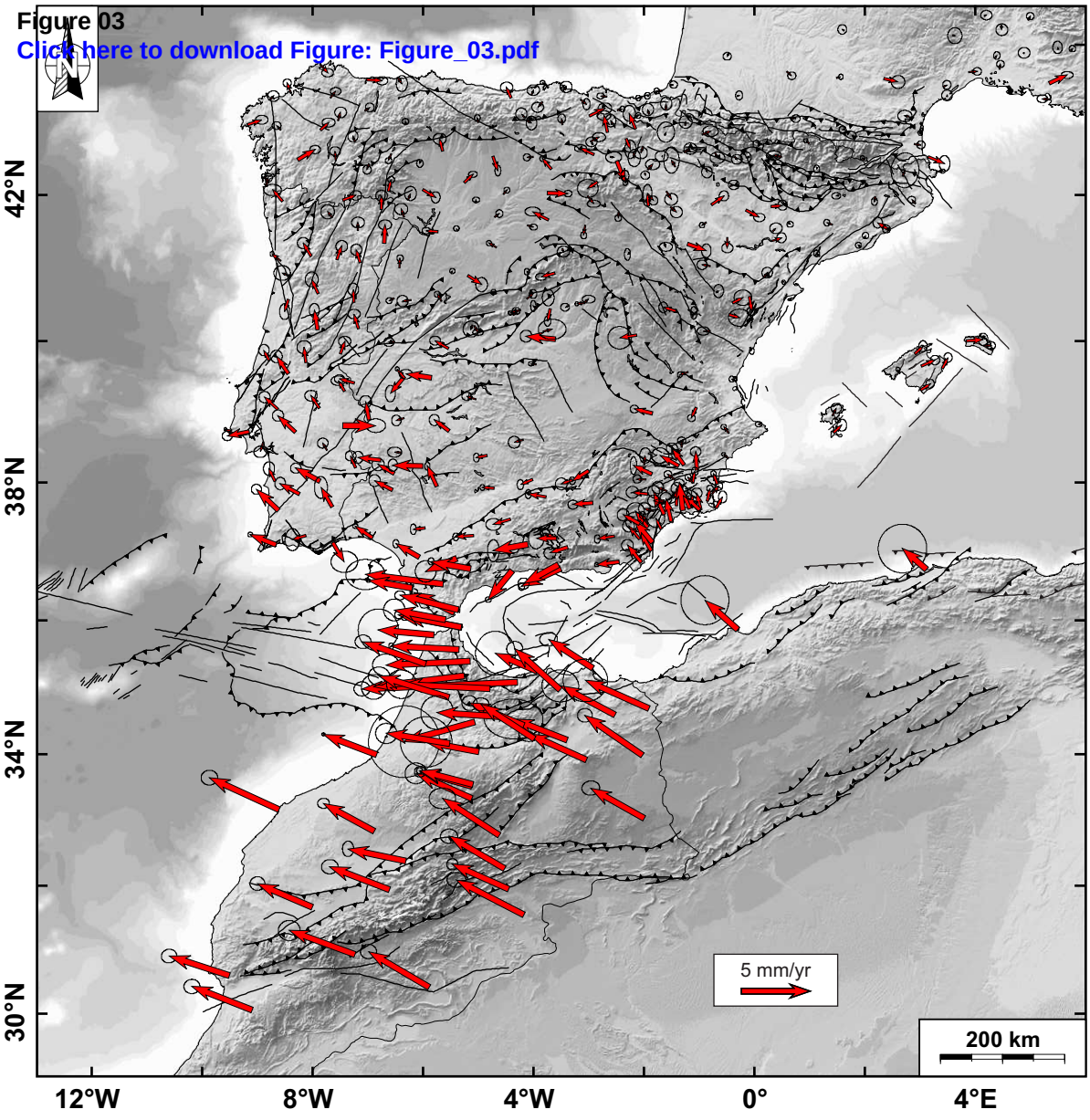

Figure 04

Click here to download Figure: Figure_04.pdf

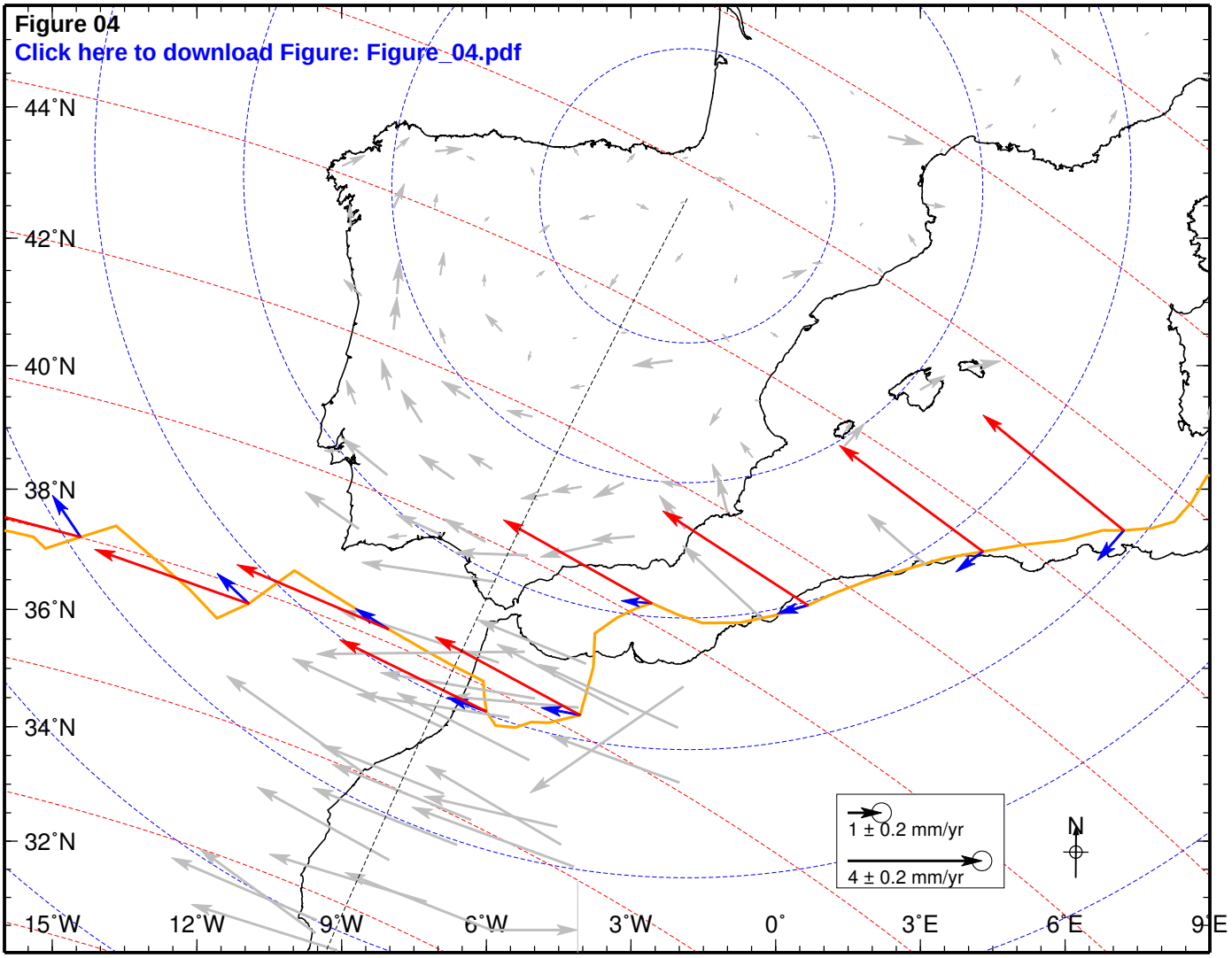

Figure 05

Click here to download Figure: Figure_05.pdf

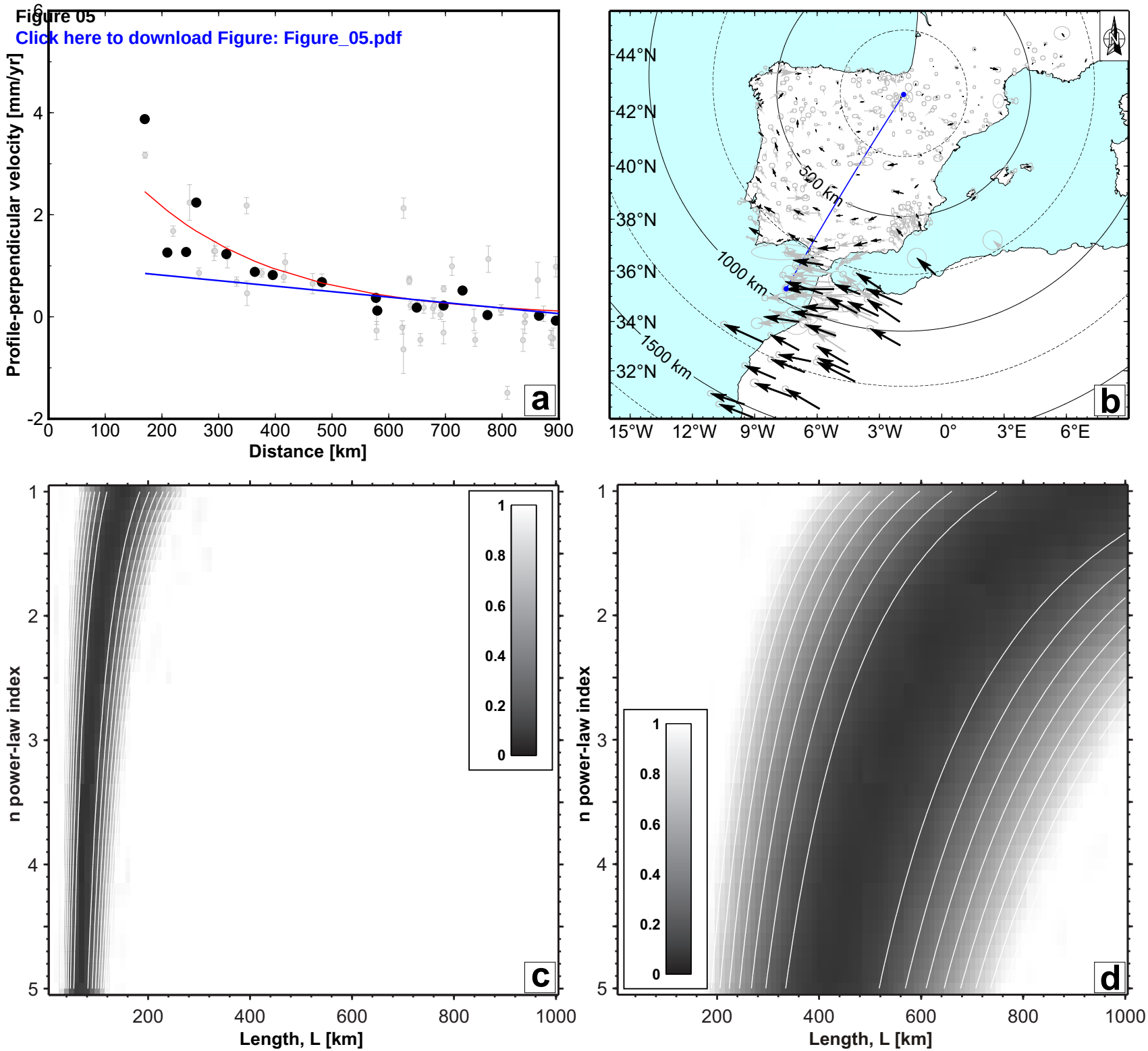

Figure 06

Click here to download Figure: Figure_06.pdf

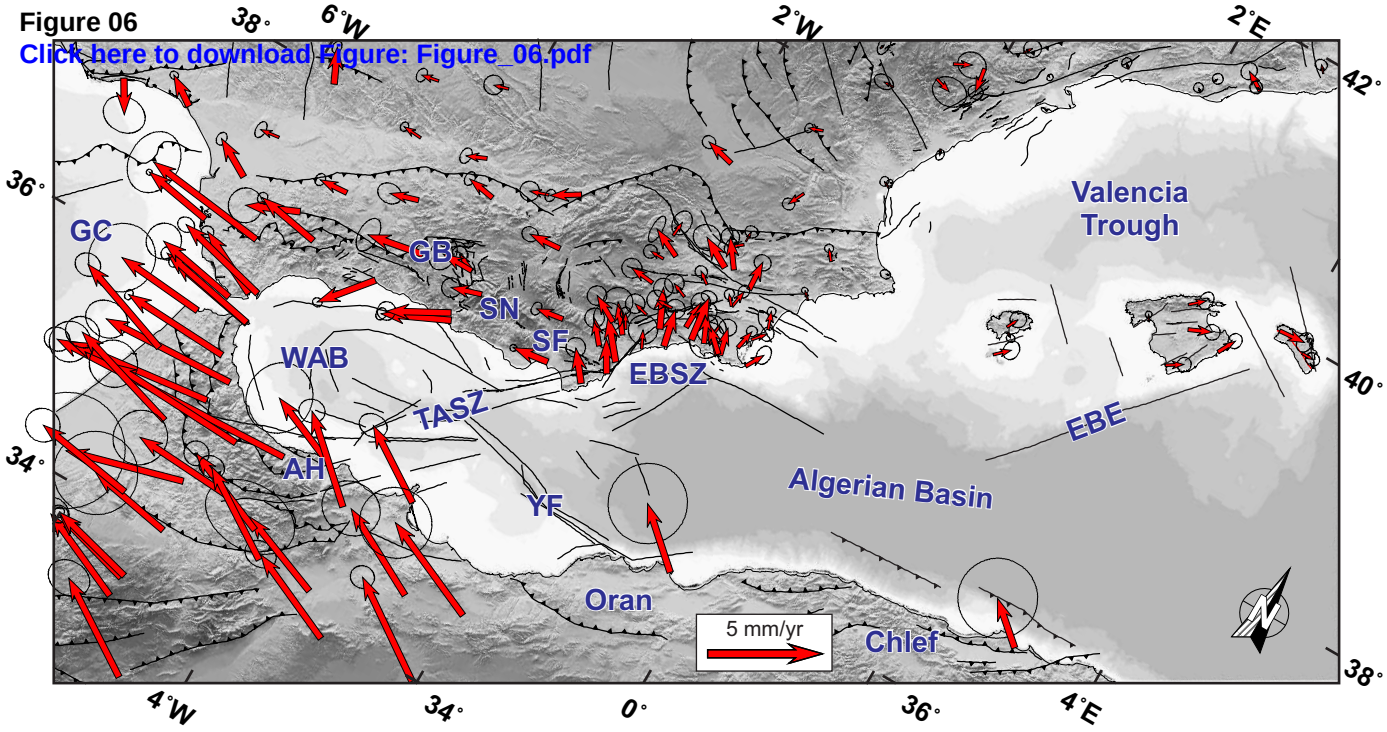

Figure 07

Click here to download Figure: Figure_07.pdf

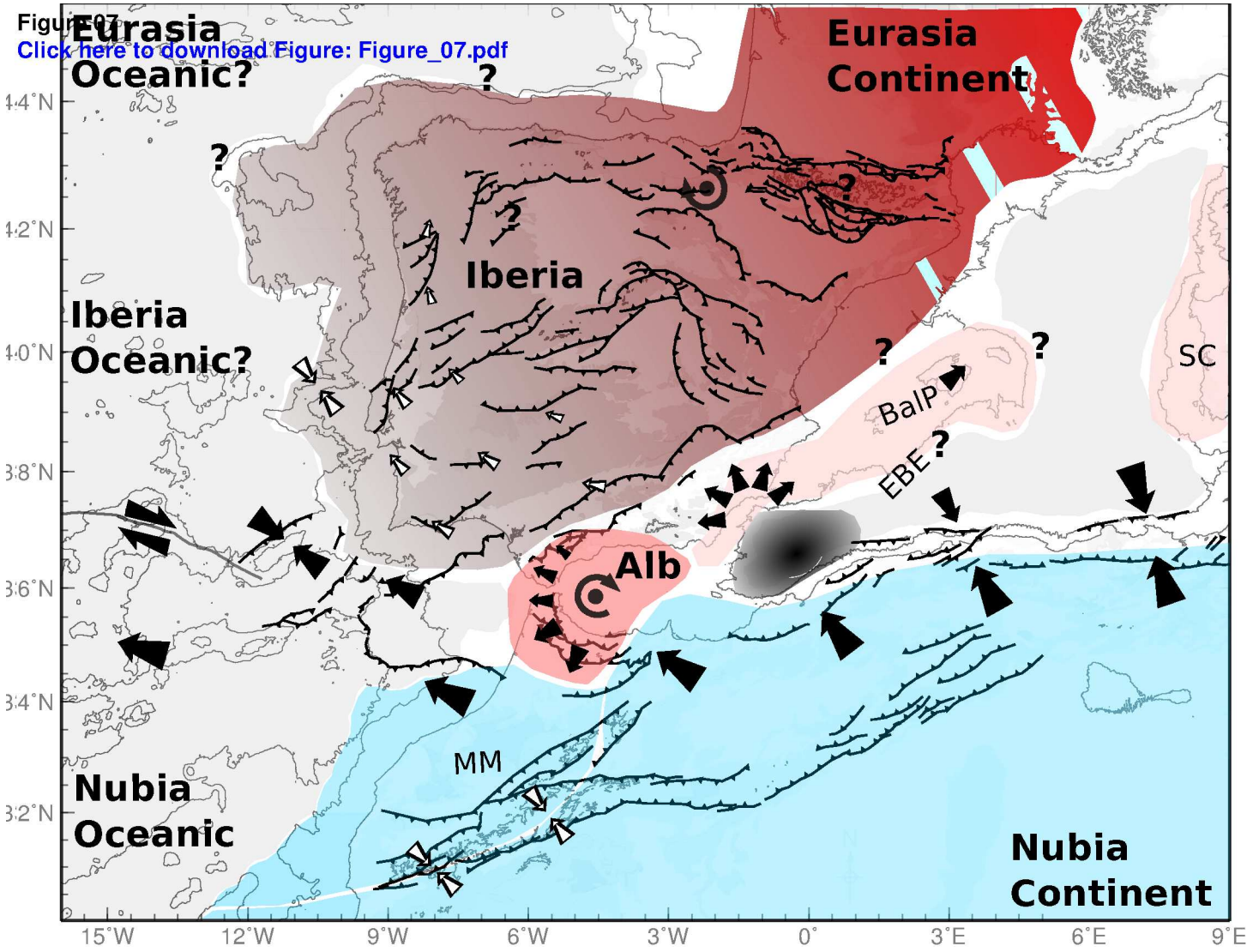

Supplementary material for online publication only

Click here to download Supplementary material for online publication only: Supplementary.Material_R2_v6.2.doc